

# Investigation of hot-carrier relaxation in quantum well and bulk GaAs at high carrier densities

W S Pelouch†, R J Ellingsont, P E Powerst, C L Tang†,  
D M Szmyd‡ and A J Nozik‡

†Materials Sciences Center, Cornell University, Ithaca, NY 14853, USA

‡Solar Energy Research Institute, 1617 Cole Boulevard, Golden, CO 80401, USA

**Abstract.** An investigation of the hot carrier relaxation in GaAs/(AlGa)As quantum wells and bulk GaAs in the high carrier density limit is presented. Using a time-resolved luminescence up-conversion technique with  $\leq 80$  fs temporal resolution, carrier temperatures are measured in the 100 fs to 2 ns range. Our results show that hot carrier cooling in quantum wells becomes significantly slower than in the bulk for carrier densities greater than  $2 \times 10^{18} \text{ cm}^{-3}$ .

It is well known that the hot carrier cooling rate decreases with increasing carrier concentration in both qw and bulk structures [1]. The first study comparing GaAs/(AlGa)As qws and bulk GaAs reported similar cooling rates at a carrier density ( $n$ ) of  $2.5 \times 10^{17} \text{ cm}^{-3}$  [2]. Subsequent studies reported a much slower cooling rate in qws than in bulk at higher carrier densities ( $n > 10^{18} \text{ cm}^{-3}$ ) [3–6]. However, recent publications [7, 8] have concluded that the cooling rates of bulk GaAs and GaAs/(AlGa)As qws are equivalent. The relative hot electron cooling rates for bulk and qw structures is an important, basic question that affects many applications of qw structures [9] and has inspired a large number of theoretical studies [10]. We have therefore re-examined this problem in the carrier density range of  $2 \times 10^{18} \text{ cm}^{-3}$  to  $1.5 \times 10^{19} \text{ cm}^{-3}$  to resolve this apparent experimental controversy.

The samples were grown by metallorganic chemical-vapour deposition on  $\langle 100 \rangle$  GaAs substrates. The bulk samples consist of (i) a 2000 Å and (ii) a 4000 Å nominally undoped GaAs layer surrounded by thin ( $< 0.2 \mu\text{m}$ ) (AlGa)As layers which are transparent to the 1.97 eV pump. The multiple quantum well structure (MQW) consists of fourteen periods of 135 Å-thick GaAs and 400 Å-thick  $\text{Al}_{0.48}\text{Ga}_{0.52}\text{As}$  grown on the GaAs substrate. The GaAs layers in the MQW contain a 3.5% Al concentration which raises the bandgap by  $\sim 50$  meV and ensures that the luminescence signal of the high-energy tail of the MQW is not confused with that of the GaAs substrate.

Time-resolved luminescence spectra were obtained by the technique of sum frequency generation [11, 12], using an arrangement nearly identical to that of [13] with the following modifications: the luminescence was collected in reflection; a 1.35 mm barium metaborate (BBO) crystal was used for up-conversion; and a cooled, low-noise (0.5 Hz dark count) Bi photomultiplier tube was used for detection. The group-velocity mismatch between the

pump and the luminescence wavelengths is 50 fs  $\text{mm}^{-1}$  in BBO and the pump pulse duration is  $\leq 50$  fs, yielding an overall temporal resolution of  $\leq 80$  fs. We calculate [14] the spectral resolution to be 10 meV.

Time-resolved luminescence spectra were recorded at room temperature for each sample at the following incident pump powers: 25 mW, 12.5 mW and 5 mW. The PL spectra of the 2000 Å bulk GaAs sample contains a contribution from the substrate at the earliest times ( $\leq 5$  ps) until the substrate carriers have diffused sufficiently. Thus results from this sample are discussed only for delays  $\geq 5$  ps. The substrate luminescence of the 4000 Å bulk GaAs is minimal. Representative spectra and carrier temperature fits for the 4000 Å bulk GaAs sample at each excitation power are shown in figure 1 for several time delays. All spectra were corrected for the spectral response of the up-conversion system. The electron temperatures were determined by fitting the high-energy tails of the spectra; only the region that is linear on a semilogarithmic plot was chosen for the fit. Figure 1(a) displays a plot of the PL spectrum at 100 fs for the highest carrier density, which shows that the initial carrier temperature is 1200 K. Figures 1(b), (c) and (d) show the evolution of the carrier distribution at time delays of 1 ps, 20 ps and 100 ps for each excitation power. The quasi-Fermi energy of the electron distribution was deduced by fitting the PL spectra and is located approximately at the position of the kink in the semilog plot of the spectra (see figure 1(c)(d)). The carrier density ( $n$ ) was calculated from the values of the quasi-Fermi levels at the highest excitation power and then scaled according to excitation power. The value of the carrier density agrees well with our calculation using beamwaist, reflection and absorption parameters; we estimate this value to be accurate to within 15%. The carrier densities for the 4000 Å GaAs sample are  $1 \times 10^{19} \text{ cm}^{-3}$ ,  $5 \times 10^{18} \text{ cm}^{-3}$  and  $2 \times 10^{18} \text{ cm}^{-3}$  corresponding to the incident excita-

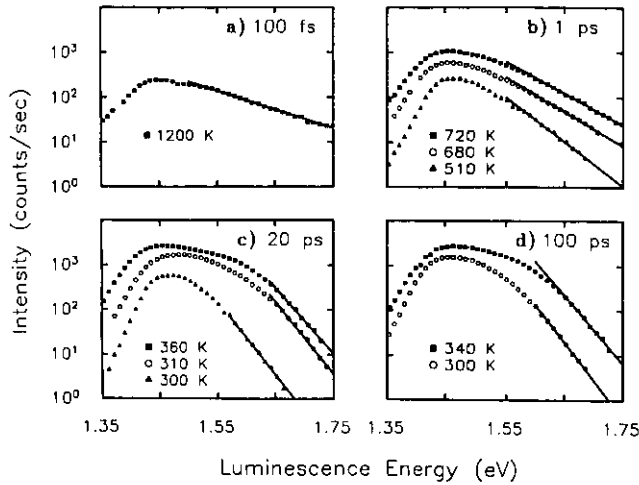


**Figure 1.** Representative time-resolved luminescence spectra for the 4000 Å bulk GaAs sample at room temperature at each excitation power (squares =  $1 \times 10^{19} \text{ cm}^{-3}$ , circles =  $5 \times 10^{18} \text{ cm}^{-3}$ , triangles =  $2 \times 10^{18} \text{ cm}^{-3}$ ). The carrier temperature fits (straight lines) and values are shown for each carrier density at delay times of (a) 100 fs, (b) 1 ps, (c) 20 ps, and (d) 100 ps.

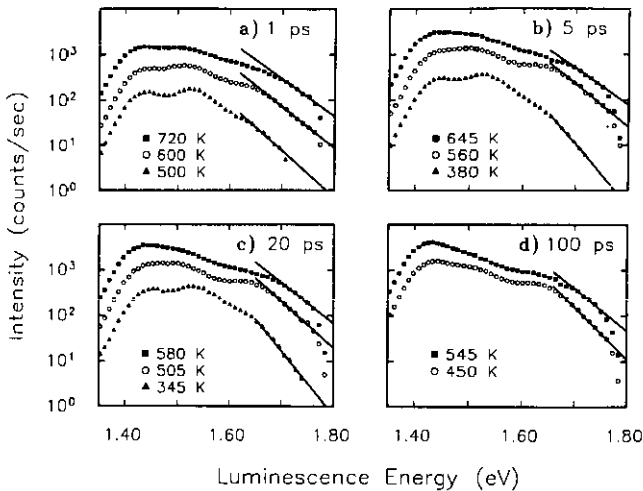


**Figure 2.** Representative time-resolved luminescence spectra for the MQW sample at room temperature at the same excitation power as the bulk (squares =  $1.4 \times 10^{19} \text{ cm}^{-3}$ , circles =  $6.8 \times 10^{18} \text{ cm}^{-3}$ , triangles =  $2.7 \times 10^{18} \text{ cm}^{-3}$ ). The carrier temperature fits (straight lines) and values are shown for each carrier density at delay times of (a) 1 ps, (b) 5 ps, (c) 20 ps, and (d) 100 ps.

tion powers of 25 mW, 12.5 mW and 5 mW, respectively. The carrier densities are 45% greater for the 2000 Å GaAs sample (PL spectra not shown).

Similarly, spectra for the MQW sample were recorded at the same pump powers as the bulk. Representative spectra and carrier temperature fits are presented in figure 2 for each excitation power. The peak at 1.43 eV corresponds to the substrate luminescence and the following peaks are attributed to the qw subbands. A small fraction of the electrons in the MQW have energies that exceed the height of the barrier potential, which can be

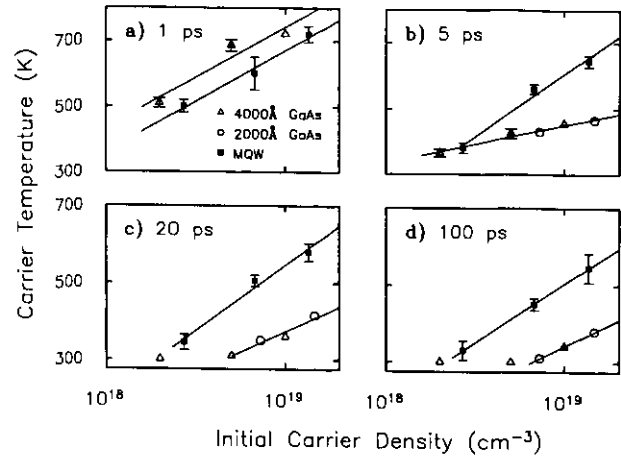


**Figure 3.** A comparison of the carrier temperatures versus initial carrier density for the 4000 Å bulk GaAs (triangles), the 2000 Å bulk GaAs (circles), and the MQW (squares) samples at time delays of (a) 1 ps, (b) 5 ps, (c) 20 ps, and (d) 100 ps. The straight lines are guides to the eye. The different dependence in carrier cooling with respect to initial carrier density between the MQW and bulk samples is most evident at intermediate times (5 ps–20 ps) and highest carrier densities.

observed as a sudden drop in the PL intensity at energies  $> 1.76 \text{ eV}$ . This fraction is less than 6% at the highest carrier density ( $< 3\%$  at the medium carrier density) and is expected to make only a minor contribution to the MQW carrier temperatures (discussed in more detail below).

The absorption coefficient at the pump wavelength in the MQW sample was measured on an etched sample and is slightly less than that of GaAs due to the 3.5% Al doping. The MQW carrier densities are calculated to be 35% greater than the 4000 Å bulk GaAs sample and 6% less than the 2000 Å GaAs sample for equal pump powers. Lineshape analysis of the mqw spectra is somewhat more difficult due to the presence of several subbands, but the measured quasi-Fermi levels yield carrier densities that agree well with the above calculations.

In figure 3 we compare the carrier temperatures of each sample versus the initial carrier density for several time delays. At 1 ps (figure 3(a)) the bulk and MQW samples have similar carrier temperatures and an identical dependence on carrier density. This represents the state of the system before an overpopulation of the phonon distribution can occur [1, 10]. In the 5 ps to 100 ps range (figure 3(b), (c), (d)) the carrier temperatures of the MQW sample remain much hotter than the bulk samples and show a substantially different dependence on initial carrier density as seen by the different slopes of the lines. In this temporal regime, the reduction in hot-carrier cooling is greatly enhanced in the MQW structure in comparison with the bulk as the carrier density increases. This is also the time scale during which the effects of a hot-phonon distribution are most evident, suggesting that this phenomenon may be due to a difference in the electron–phonon interplay in quasi-2D and 3D systems, which becomes evident at high carrier densities. The carrier temperature of the 4000 Å bulk

GaAs sample has cooled to 310 K by 2000 ps (not shown) at the highest carrier density.

It must be noted that the carriers in the MQW sample are excited only within the well region, but at energies above the conduction band that exceed the height of the barrier potential. Since the holes are bound within the quantum well at all times, the electrons are initially trapped in the unbound states of the QW due to Coulomb attraction [15] until they are bound in the well by energy loss via phonon emission ( $< 1$  ps). Any carriers that happen to diffuse to the barrier region would also return to the QW within a few picoseconds [15,16]. It is reasonable to expect that these effects could not account for the slowed QW carrier cooling which occurs on a time scale of hundreds of picoseconds. Thus we do not believe carrier diffusion can account for the vast differences between MQW and bulk carrier cooling that we observe.

These data show that the hot-carrier cooling is intrinsically different in quasi-2D and 3D systems at higher carrier densities ( $n > 10^{18} \text{ cm}^{-3}$ ). The experiment described in this paper represents a significant improvement over the previous methods in the ability to characterize the evolution of the hot-carrier distribution. Unlike nonlinear intensity correlation experiments [2,3] the state of the system can evolve without perturbation after the pump (i.e., there is no probe). The method of luminescence detection using a streak camera [7,8] lacks the ability to detect hot luminescence for times less than or of the order of the phonon lifetime due to the limited temporal resolution, which requires the experiment to be carried out at low temperatures in order to observe any effects of the hot-carrier relaxation. The results of these previous studies agree with our observations in their respective carrier density ranges. The similarity in the cooling rates of MQW and bulk GaAs at  $n = 2 \times 10^{18} \text{ cm}^{-3}$ , as seen in figure 3, suggests that these cooling rates would be nearly identical at lower carrier concentrations, in agreement with [2,7,8]. It should also be noted that we have observed that the precise values of the carrier temperatures of a variety of MQW samples depend on both sample quality and age (the latter presumably due to degradation of the samples with oxidation of the (AlGa)As surface), but the qualitative results of this study are not affected.

In conclusion, the hot-carrier cooling rates in GaAs/(AlGa)As quantum wells and bulk GaAs have been investigated in the high carrier density limit ( $n \geq 2 \times 10^{18} \text{ cm}^{-3}$ ). The cooling rates of the quantum

well structure are significantly slower than that of the bulk for  $n \geq 5 \times 10^{18} \text{ cm}^{-3}$  and similar at  $n = 2 \times 10^{18} \text{ cm}^{-3}$ , in agreement with the results of previous publications. The investigation of hot-carrier relaxation in the high carrier density limit is important in order to understand the physics governing quasi-2D and 3D hot-carrier relaxation over the widest range of conditions and may have important consequences in the development of semiconductor devices.

## Acknowledgments

The research at Cornell was supported by the Joint Services Electronics Program and the National Science Foundation. AJN and DMS were supported by the US Department of Energy, Division of Basic Energy Sciences/Chemical Sciences.

## References

- [1] Shah J 1989 *Solid-State Electron.* **32** 1051 and references therein
- [2] Shank C V, Fork R L, Yen R, Shah J, Greene B I, Gossard A C and Weisbuch C 1983 *Solid State Commun.* **47** 981
- [3] Xu Z Y and Tang C L 1984 *Appl. Phys. Lett.* **44** 692
- [4] Ukichi H, Arakawa Y, Sakaki H and Kobayashi T 1985 *Solid State Commun.* **55** 311
- [5] Lyon S A 1986 *J. Lumin.* **35** 121
- [6] Nozik A J, Parsons C A, Dunlavy D J, Keyes B M and Ahrenkiel R K 1990 *Solid State Commun.* **75** 297
- [7] Leo K, Rühle W W and Ploog K 1988 *Phys. Rev.* **B 38** 1947; 1989 *Solid-State Electron.* **32** 1863
- [8] Leo K, Rühle W W, Queisser H J and Ploog K 1988 *Appl. Phys.* **A 45** 35; 1988 *Phys. Rev.* **B 37** 7121
- [9] See for example 1990 *High Speed Semiconductor Devices* ed S M Sze (New York: Wiley)
- [10] See for example Lugli P and Goodnick S M 1987 *Phys. Rev. Lett.* **59** 716
- [11] Mahr H and Hirsch M D 1975 *Opt. Commun.* **13** 96
- [12] Damen T C and Shah J 1988 *Appl. Phys. Lett.* **52** 1291
- [13] Wise F W and Tang C L 1989 *Solid State Commun.* **69** 821
- [14] Shah J 1988 *IEEE J. Quantum Electron.* **QE-24** 276
- [15] Devaud B, Shah J, Damen T C and Tsang W T 1988 *Appl. Phys. Lett.* **52** 1886
- [16] Bimberg D, Christen J, Stechenborn A, Weimann G and Schlapp W 1985 *J. Lumin.* **30** 562  
Westland D J, Mihailovic D, Ryan J F and Scott M D 1987 *Appl. Phys. Lett.* **51** 590